Short communication

Electrochemical synthesis of macroporous aluminium films and their behavior towards lithium deposition/stripping

L.H.S. Gasparotto [a,b], A. Prowald [b], N. Borisenko [a,b], S. Zein El Abedin [a,b,c], A. Garsuch [d], F. Endres [a,b,*]

[a] Institute of Particle Technology, Arnold-Sommerfeld-Strasse 6, D-38678 Clausthal-Zellerfeld, Germany
[b] EFZN Goslar, Am Stollen 19, D-38640 Goslar, Germany
[c] Electrochemistry and Corrosion Laboratory, National Research Centre, Dokki, Cairo, Egypt
[d] BASF, Ludwigshafen, Germany

ABSTRACT

In the present study macroporous aluminium electrodes were made by template assisted electrodeposition from ionic liquids. Polystyrene (PS) spheres (diameter 600 nm) were applied onto polished copper electrodes by immersion into an alcoholic suspension containing PS spheres. Al was deposited from the chloroaluminate ionic liquid [EMIm]Cl/AlCl$_3$ (40/60 mol.%) on this substrate. After chemical dissolution of the PS spheres a macroporous aluminium electrode was obtained which served as a host material for Li deposition from ionic liquids. Lithium deposition in this matrix is reversible showing certain activation with an increasing number of cycles. After 10 cycles of Li deposition/dissolution the macroporous structure is still visible.

© 2010 Elsevier B.V. All rights reserved.

1. Introduction

Aluminium is an attractive anode material for Li ion batteries due to the high specific energy and low cost [1]. However the large volume expansion/contraction during Al–Li alloying causes aluminium cracking and a gradual degradation, resulting in a fast capacity fading and a poor cyclability [2]. Intermetallic materials such as Al$_2$Cu, AlSb and Fe$_2$Al$_5$ have been regarded as candidates to overcome these problems [3,4], but their first charge/discharge capacities (20–40%) are rather disappointing. The potential of metal oxides as high-capacity anodes has also been investigated [5,6]. One major drawback is still the large volume expansion during Li intercalation in case of corresponding compounds. There are other promising candidates for anodes in lithium ion batteries such as Si, Ge and Sn, as they have high capacities. However, they also show a drastic volume change associated with the insertion/extraction of lithium, resulting in poor cyclic performance [7–9]. Attempts have been made to overcome the volume change using nanostructured materials. Cui and coworkers have indicated that anodes made of Si [10] or Ge [11] nanowires were able to allow for the large volume changes without pulverization or loss of contact. The interstitial spaces in the nanowires facilitate the accommodation of

the volume changes and provide more access sites for Li ions. Quite recently aluminium anodes comprising free standing Al-nanorods have demonstrated high capacities and a good cycleability [12].

The use of macroporous aluminium (MP-Al) deposited directly on the current collector might offer a further solution to the above-mentioned problems. Firstly, this structure may reduce the stress from the charge/discharge process as its macroporous nature might accommodate the volume expansion. Secondly, the electronic conductivity might be improved due to the direct contact of the MP-Al with the current collector.

In this paper we present our first results on the fabrication and characterization of a macroporous aluminium matrix electrodeposited from an ionic liquid consisting of 1-ethyl-3-methylimidazolium choride ([EMIm]Cl) and AlCl$_3$ (40/60 mol.%) using a polystyrene (PS) sphere template. Electrodeposition of aluminium from chloroaluminate ionic liquids was extensively investigated, see for example [13–16]. Macroporous structures of CdS [17], CdSe [18], and conducting polymers [19] are known to be accessible by a template-assisted electrochemical deposition process. Furthermore it was shown that macroporous structures of Ge and Si$_x$Ge$_{1-x}$ [20] can be made by electrodeposition from ionic liquids. In contrast to other methods (e.g. chemical vapor deposition [21] and sol–gel techniques [22]), which are top-down processes filling only the top few layers, the electrochemical one ensures a high density of the deposited materials as the deposition occurs in the space between the template spheres filling from the bottom of the electrode to the top. In a previous study on germanium macroporous structures [23] we discussed that the usually very low surface

---

tensions of ionic liquids (about 20–30 mN m^{-1}) facilitate wetting of the template electrode and consequently the deposition process from the bottom of the electrode.

In this paper we present the fabrication of a macroporous Al electrode. SEM/EDX investigations before Li deposition and after a number of Li plating/stripping cycles give insight about the mechanical stability of the host material when used for lithium storage. Other elements (Si, Ge, Sn) and maybe alloys might allow to taylor macroporous electrode materials.

2. Experimental

A copper sheet (1 cm × 5 cm) was used as substrate for macroporous electrodes. Before preparation the copper was polished with abrasive paper (grain size 1 μm) and washed in acetone and isopropanol. Polystyrene (PS) spheres with 600 nm diameter (Duke Scientific) were suspended in pure ethanol (10 vol% PS in ethanol). For electrode preparation the copper sheet was dipped at 38 °C in the polystyrene suspension and pulled out. It was observed, that the PS spheres self-assembled on the copper surface mainly in an ordered hexagonal structure. Before use as an electrode for Al deposition the PS-covered copper was tempered at 100 °C for 2 h leading to a better attachment of the spheres.

All electrochemical experiments were performed in an argon-filled glove box with water and oxygen contents of below 2 ppm (OMNI-LAB from Vacuum-Atmospheres). [EMIm]Cl/AlCl$_3$ (40/60 mol.%) ionic liquid was made by careful mixing of both components under inertgas. The macroporous aluminium (MP-Al) was made as follows: a cylinder made from PTFE was pressed onto the PS-covered copper sheet resulting in an electrochemical cell with a geometric surface area of 0.3 cm^2. The PS-covered copper electrode served as working electrode. An Al-wire and an Al-ring (99.99%) were polished with emery paper and used as reference and counter electrodes, respectively. For Al deposition the electrochemical cell was filled with the [EMIm]Cl/AlCl$_3$ ionic liquid and an electrode potential of −0.5 V vs. Al was applied for 3 min using a PARSTAT 2263 potentiostat/galvanostat controlled by the Power-Suite software. After Al deposition the main part of [EMIm]Cl/AlCl$_3$ ionic liquid was removed from the electrochemical cell with a Pasteur pipette. The cell was subsequently rinsed with pure 1-butyl-1-methylpyrrolidinium bis(trifluoromethylsulfonyl) amide ([Py$_{1,4}$]TFSA) ionic liquid to remove any remaining [EMIm]Cl/AlCl$_3$. It is of eminent importance to remove the AlCl$_3$ containing liquid inside the glove box. Otherwise HCl is formed under air leading to a strong attack of the macroporous Al. Furthermore solid hydrolysis products might fill the pores. [Py$_{1,4}$]TFSA efficiently removes AlCl$_3$ and it can be finally removed by rinsing with isopropanol, resulting in a reproducible material. The PS template was chemically removed by tetrahydrofuran (THF) treatment to yield the aluminium macroporous structure. A solution consisting of 0.5 mol l^{-1} LiTFSA in [Py$_{1,4}$]TFSA was used for lithium electrodeposition/-dissolution experiments employing the MP-Al electrode. For these experiments, a Pt-wire and a Pt-ring (99.99%) were used as quasi-reference and counter electrodes, respectively.

For SEM-EDX investigations a high resolution scanning electron microscope (Carl Zeiss DSM 982 Gemini) with energy dispersive X-ray analyzer was utilized. The PS coated electrodes were sputtered with platinum for scanning electron microscopy (SEM) imaging.

3. Results

3.1. Preparation of the polystyrene template

Mono-sized polystyrene spheres (600 nm) are able to form hexagonal ordered three dimensional structures by self-assembly.
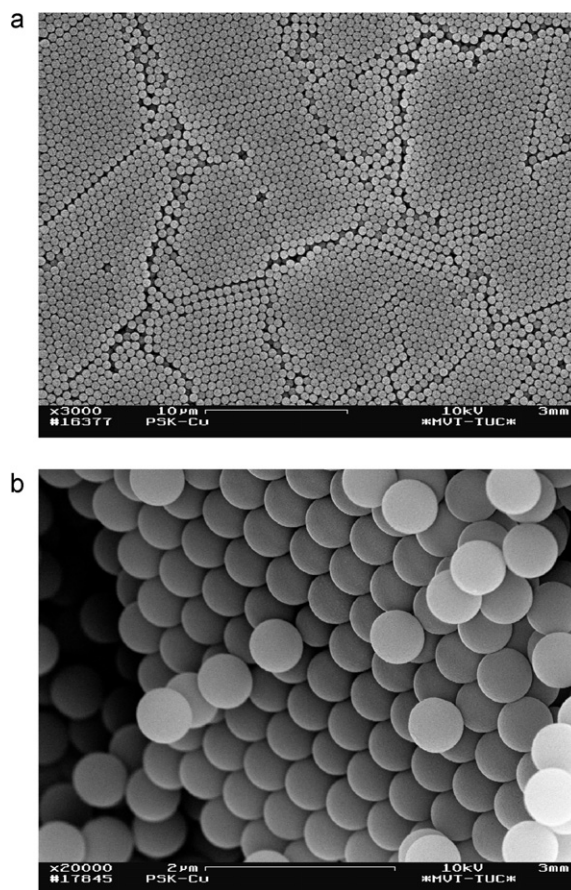
Fig. 1. (a) Polished Cu electrode with hexagonal ordered polystyrene template (600 nm diameter) on top, and (b) cross section reveals nine polystyrene layers.

This characteristic makes them suitable as a matrix for the synthesis of macroporous electrodes. Fig. 1 shows a SEM image of a polished copper sheet with PS spheres on top. The PS spheres arrange well on the polished electrode, but due to the electrode surface roughness (resulting from polishing) the PS layer exhibits some disordered domains within the hexagonal ordered structure. A view on the cross-section (Fig. 1b) shows that with this simple dipping process up to 9 ordered layers can be obtained in one step. For comparison purposes, a SEM image of Au(1 1 1) covered with PS spheres is displayed in Fig. 2. By looking at both images (Figs. 1 and 2) it is obvious that more defects exist in case of the PS layer on the rough copper surface.

3.2. Preparation of the macroporous aluminium electrode

Fig. 3 shows a cyclic voltammogram of the copper electrode covered with the PS template in [EMIm]Cl/AlCl$_3$ at a scan rate of 10 mV s^{-1} at room temperature. The potential was scanned from the open circuit potential (0.8 V vs. Al) to the negative direction until −0.6 V. The aluminium bulk deposition starts at about −0.15 V. In the cathodic part of the back scan, the current values are higher than those recorded in the forward scan (with a current loop) at the same potential, which is indicative for a process involving nucleation and growth of aluminium on the Cu electrode. The anodic peak at 0.56 V is correlated with the stripping of the formerly electrodeposited aluminium. The magnitude of the recorded currents indicates that the [EMIm]Cl/AlCl$_3$ easily wets the copper substrate by the interstices of the close-packed PS template. The low surface tension of ionic liquids facilitates wetting of the Cu surface. Fig. 4 shows SEM images of the macroporous aluminium (after removal
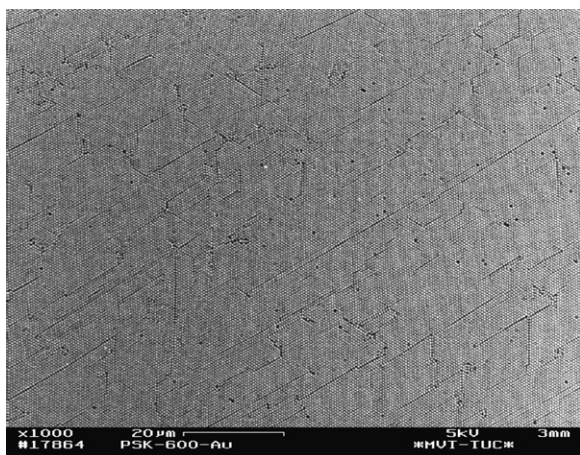
Fig. 2. Au(1 1 1) electrode with hexagonal ordered polystyrene template on top. The structure on the single crystalline surface is much better ordered than on the polished copper.

of the PS spheres with THF) obtained at a constant potential of −0.5 V for 3 min at room temperature. Fig. 4a reveals a well-covered porous surface with some disordered areas (indicated by the circles), where aluminium rather grew as a closed film. These sites might be the result of an imperfect PS template and/or of uneven current densities inside the electrochemical cell. EDX measurements reveal oxygen besides aluminium, a consequence of the *ex situ* handling of the macroporous electrode. The rows indicated by the white arrows represent the polishing traces of the Cu underneath. A higher-magnification picture (Fig. 4b) shows an ordered macroporous nanoarchitecture consisting of spherical pores. The layers underneath are also visible revealing the three-dimensional structure. In our opinion template-assisted electrodeposition from ionic liquids is a simple way to obtain macroporous materials.

3.3. Lithium deposition on macroporous aluminium

Ionic liquids containing the TFSA anion have been intensely studied as electrolytes for lithium rechargeable batteries because of their non-volatility and non-flammability [24–27]. Furthermore, the extension of the cathodic limit in these ionic liquids upon addition of a lithium salt has been reported [24,28,29] allowing reversible Li deposition/dissolution. The suitability of ionic liquids for use in lithium batteries is discussed in literature and a recent article by Scrosati and Garche points out the improvements in
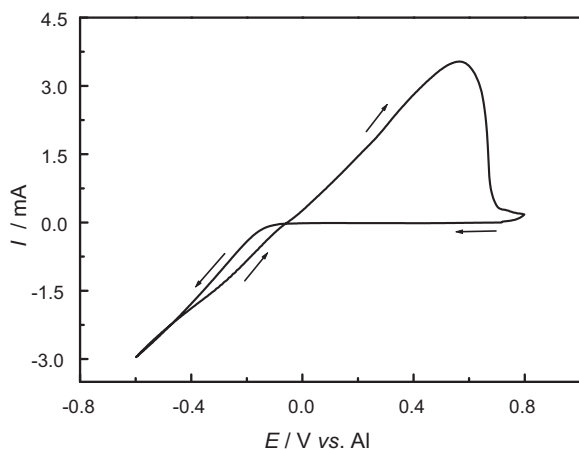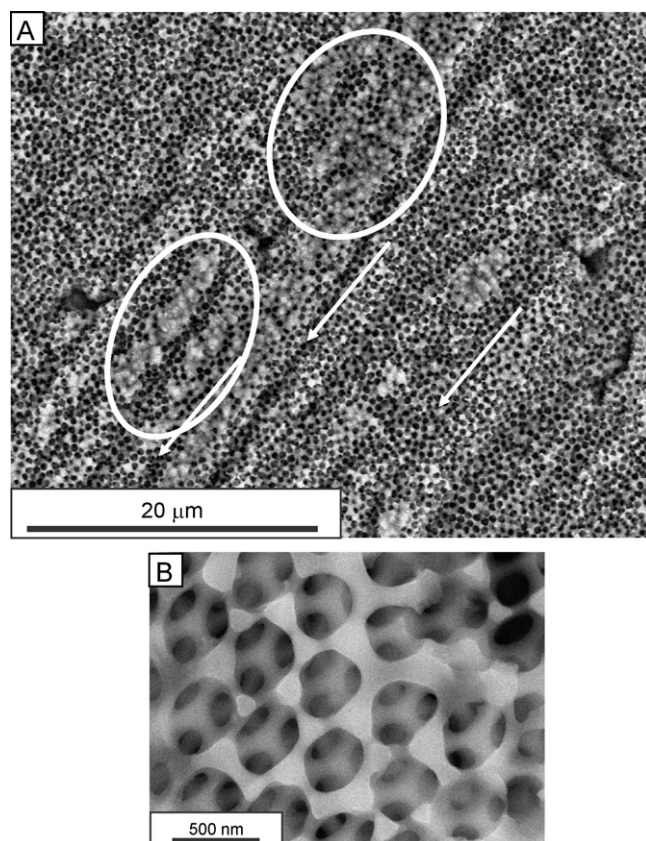

Fig. 4. SEM images of the macroporous Al obtained at −0.5 V *vs.* Al for 3 min in [EMIm]Cl/AlCl$_3$. $\theta = 25\,^\circ$C.

safety and reliability for lithium batteries employing ionic liquids [30]. Fig. 5 shows the first 10 CVs for the macroporous Al electrode in [Py$_{1,4}$]TFSA containing 0.5 mol l^{-1} LiTFSA at a scan rate of 10 mV s^{-1} at room temperature. The potential was scanned in the negative direction from −1 V down to −4 V *vs.* Pt. As seen in Fig. 5, the electrodeposition of Li starts at about −3.1 V. The anodic peak centered at −2.4 V *vs.* Pt is attributed to lithium dissolution. In the first 2 cycles the beginning deposition and the oxidation peaks are a bit shifted. This might be a hint for Li/Al alloying [12]. With an increasing number of cycles the anodic charge also increases. This activation might be due to alloying/dealloying or due to some oxide coverage on the Al surface. Even under the conditions of an inertgas glove box traces of oxygen could not totally be prevented.
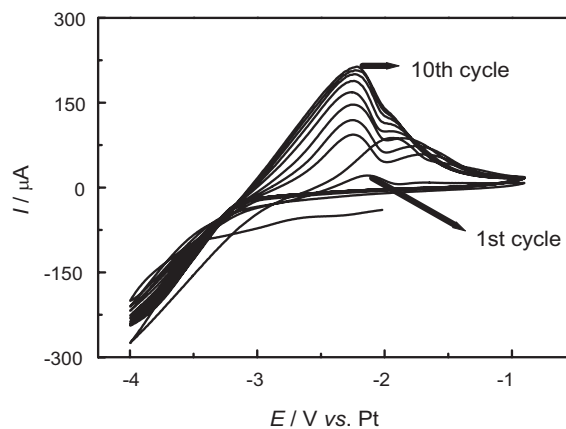

Fig. 3. Cyclic voltammogram for the Cu/polystyrene template electrode in [EMIm]Cl/AlCl$_3$. Scan rate: 10 mV s^{-1}. $\theta = 25\,^\circ$C and $A = 0.3$ cm^2.

Fig. 5. Cyclic voltammograms for the macroporous Al electrode in [Py$_{1,4}$]TFSA + 0.5 mol l^{-1} LiTFSA. Scan rate: 10 mV s^{-1}. $\theta = 25\,^\circ$C.
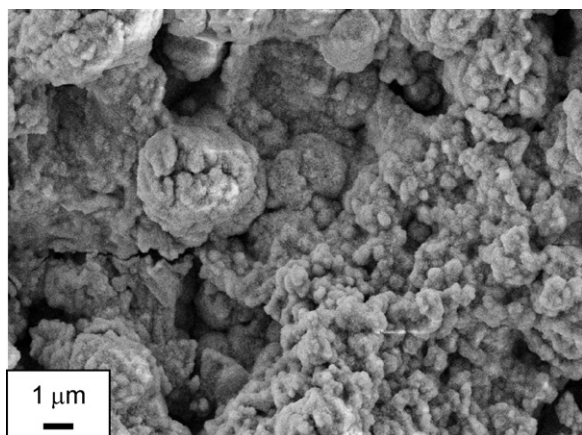
Fig. 6. SEM image of Li deposit on macroporous Al obtained by applying a cathodic current of 0.25 mA for 30 min.

With subsequent cycling the active area for lithium deposition is increased and in the 9th and 10th cycles there is practically no more difference between the anodic currents. If a cathodic current of 0.25 mA is applied for 30 min (which leads to an overloading with Li) the whole of the macroporous Al electrode is covered with a massive Li film (Fig. 6).

In order to find out how lithium deposition/dissolution affects the macroporous aluminium electrode, we investigated the electrode after Li deposition/dissolution with SEM. Fig. 7 presents an image of the MP-Al electrode after the first voltammetric cycle in $[Py_{1,4}]TFSA + 0.5 \, mol \, l^{-1}$ LiTFSA. A full voltammetric cycle comprises lithium deposition and its complete dissolution. As can be seen the macroporous structure is retained. Au et al. [12] observed blurred SEM images of the aluminium nanorods after the first lithium deposition/oxidation cycle in their studies on Al nanorods as anodes for batteries. They attributed this result to either Al oxidation (due to exposure to air) or to a loss of contact of the Al nanorods with the Ti substrate. In our work the macroporous Al was also exposed to air during the cleaning procedure, however the SEM images after the first voltammetric cycle were well resolved, which implies that the macroporous Al was in a good contact with the Cu substrate. At the first glance our macroporous Al shows an
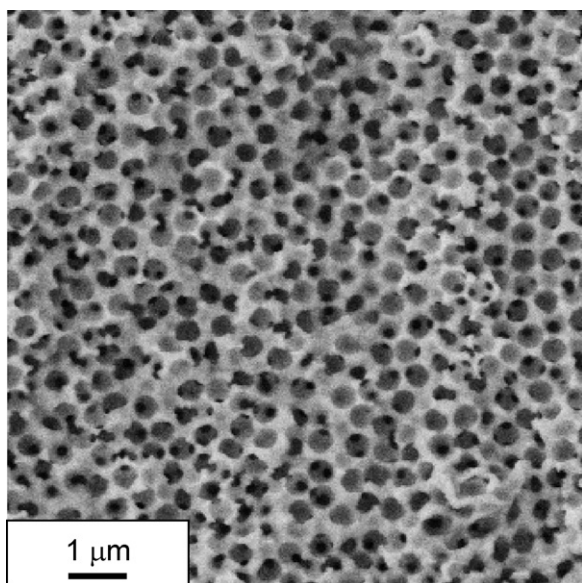

Fig. 7. SEM image of macroporous Al after the first voltammetric cycle in $[Py_{1,4}]TFSA + 0.5 \, mol \, l^{-1}$ LiTFSA.

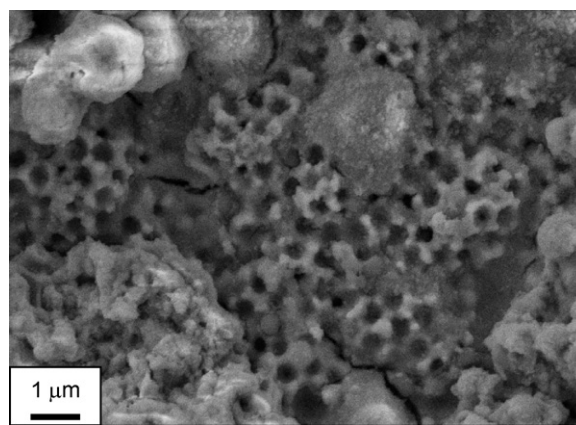**Fig. 8.** SEM image of macroporous Al after 10 voltammetric cycles in $[Py_{1,4}]TFSA + 0.5 \, mol \, l^{-1}$ LiTFSA.

enhanced stability. However, after the tenth voltammetric cycle the macroporous Al changes its morphology as shown in Fig. 8. The porous structure is still visible, but it is no longer as continuous as after the first cycle and regions with lithium agglomerates have appeared. Nevertheless the electrode is electrochemically still quite active. We assume that the mechanical stress during the quite fast deposition/dissolution accompanied with alloying/dealloying leads to a partial disintegration of the macroporous host material. It would be of interest to investigate the effects of the scan rate on the morphology of the macroporous electrode. Furthermore it is of interest to test other elements and alloys for their suitability as macroporous electrodes for lithium storage.

In the light of the aforementioned results it can be concluded that the macroporous aluminium can be regarded as a promising anode material for lithium (ion) batteries. An alloying between lithium and aluminum has to be expected; furthermore the deposition of pure Li takes place in the voids of the Al structure. The gravimetric capacities for LiAl and Li are 790 mAh g^{-1} and 3862 mAh g^{-1}, respectively. As the packing density of the PS spheres is around 74%, 26% of the electrode's volume is available for alloying, which gives theoretical volumetric capacity of 332.8 mAh cm^{-3} for LiAl. For pure Li, 74 vol% is available, giving 1525.14 mAh cm^{-3}. The actual electrode's capacities should be between those of LiAl and pure Li, which are much higher than those of lithiated graphite (372 mAh g^{-1} and 837 mAh cm^{-3}) [31]. The porous structure of the synthesized aluminium enhances the accommodation of Li metal inside the pores without the formation of dendrites. A detailed characterization of the synthesized macroporous Al electrodes will be given in a future paper.

4. Conclusion

We have presented our first results on the facile synthesis and characterization of a macroporous aluminium (MP-Al) electrode. MP-Al has been successfully obtained by a template-assisted electrochemical method from the chloroaluminate ionic liquid [EMIm]Cl/AlCl$_3$ (40/60 mol.%). The MP-Al electrode was used as a host substrate for Li deposition from the ionic liquid $[Py_{1,4}]TFSA$ containing LiTFSA. Upon lithium deposition/oxidation on MP-Al, the macroporous structure remains intact after the first voltammetric cycle. However, after 10 cycles, the ordered macroporosity is partially lost and agglomerated structures emerge.

Acknowledgements

References

[1] Q. Li, N.J. Bjerrum, J. Power Sources 110 (2002) 1.
[2] M. Winter, J.O. Besenhard, Electrochim. Acta 45 (1999) 31.
[3] D. Larcher, L.Y. Beaulieu, O. Mao, A.E. George, J.R. Dahn, J. Electrochem. Soc. 147 (2000) 1703.
[4] M.J. Lindsay, G.X. Wang, H.K. Liu, J. Power Sources 119–121 (2003) 84.
[5] N. Li, C.R. Martin, B. Scrosati, J. Power Sources 97–98 (2001) 240.
[6] Y.-M. Kang, K.-T. Kim, J.-H. Kim, H.-S. Kim, P.S. Lee, J.-Y. Lee, H.K. Liu, S.X. Dou, J. Power Sources 133 (2004) 252.
[7] H.Y. Lee, S.M. Lee Wu, Electrochem. Commun. 6 (2004) 465.
[8] M. Winter, J.O. Bsenhard, Electrochim. Acta 45 (2000) 31.
[9] Z. Gu, Y. Han, F. Pan, X. Wang, D. Weng, S. Zhou, Mater. Sci. Forum 610–613 (2009) 467.
[10] C.K. Chan, H. Peng, G. Lin, K. McIlwrath, X.F. Zhang, R.A. Huggins, Y. Cui, Nat. Nanotechnol. 3 (2008) 31.
[11] C.K. Chan, X.F. Zhang, Y. Cui, Nano Lett. 8 (2008) 307.
[12] M. Au, S. McWhorter, H. Ajo, T. Adams, Y. Zhao, J. Gibbs, J. Power Sources 195 (2010) 3333.
[13] C.L. Hussey, Pure Appl. Chem. 60 (1988) 1763.
[14] G.R. Stafford, J. Electrochem. Soc. 141 (1994) 245.
[15] Y. Zhao, T.J. VanderNoot, Electrochim. Acta 42 (1997) 1639.
[16] Q.X. Liu, S. Zein El Abedin, F. Endres, Surf. Coat. Technol. 201 (2006) 1352.
[17] P.V. Braun, P. Wiltzius, Adv. Mater. 13 (2001) 482.
[18] P.V. Braun, P. Wiltzius, Nature 402 (1999) 603.
[19] T. Sumida, Y. Wada, T. Kitamura, S. Yanagida, Chem. Commun. (2000) 1613.
[20] R. Al Salman, X. Meng, J. Zhao, Y. Li, U. Kynast, M.M. Lezhnina, F. Endres, Pure Appl. Chem. 82 (8) (2010) 673.
[21] A. Blanco, E. Chomski, S. Grabtchak, M. Ibisate, S. John, S.W. Leonard, C. Lopez, F. Meseguer, H. Miguez, J.P. Mondia, G.A. Ozin, O. Toader, H.M. van Driel, Nature 405 (2000) 437.
[22] R.W.J. Scott, S.M. Yang, G. Chabanis, N. Coombs, D.E. Williams, G.A. Ozin, Adv. Mater. 13 (2001) 1468.
[23] X.D. Meng, R. Al-Salman, J.P. Zhao, N. Borissenko, Y. Li, F. Endres, Angew. Chem. Int. Ed. 48 (2009) 2703.
[24] Y. Katayama, T. Morita, M. Yamagata, T. Miura, Electrochemistry 71 (2003) 1033.
[25] P.C. Howlett, D.R. MacFarlane, A.F. Hollenkamp, J. Power Sources 114 (2003) 277.
[26] H. Sakaebe, H. Matsumoto, Electrochem. Commun. 5 (2003) 594.
[27] B. Garcia, S. Lavallee, G. Perron, C. Michot, M. Armand, Electrochim. Acta 49 (2004) 4583.
[28] P.C. Howlett, D.R. MacFarlane, A.F. Hollenkamp, Electrochem. Solid State Lett. 7 (2004) A97.
[29] H. Matsumoto, H. Kageyama, Y. Miyazaki, Electrochemistry 71 (2003) 1058.
[30] B. Scrosati, J. Garche, J. Power Sources 195 (2010) 2419.
[31] W.-J. Zhang, J. Power Sources 196 (2011) 13.